TÜBİTAK

Turkish Journal of Chemistry

http://journals.tubitak.gov.tr/chem/

Research Article

Turk J Chem
(2018) 42: 1534 – 1543
© TÜBİTAK
doi:10.3906/kim-1805-37

Determination of morin on an electrochemically activated carbon-paste electrode

Alexander CHEBOTAREV, Konstantin PLIUTA, Denys SNIGUR*
Department of Analytical Chemistry, Faculty of Chemistry, Odessa I. I. Mechnikov National University, Odessa, Ukraine

Received: 16.05.2018 • **Accepted/Published Online:** 11.07.2018 • **Final Version:** 06.12.2018

Abstract: In this paper, the possibility of using an electrochemically activated carbon-paste electrode (ECA-CPE) for the determination of morin has been studied. It is established that the oxidation current increases 1.85 times in comparison with untreated CPE. The adsorption nature of the anodic current and the number of electrons taking part in the oxidation of morin on ECA-CPE was established. The optimal conditions for the determination of morin (pH = 4, E_{ads} = 200 mV, t_{ads} = 180 s) were established. Using square-wave voltammetry (A = 35 mV, ν = 25 Hz, υ = 100 mV/s) it is possible to determine morin in the range of concentrations of 6–0.8 µM (with 0.314 µA/µM sensitivity) and 0.8–0.16 µM (with 0.557 µA/µM sensitivity). The developed sensor was tested for the determination of morin in model solutions and *Coffea arabica* extracts with RSD lower than 4.5%.

Key words: Carbone-paste electrode, electrochemical activation, morin

1. Introduction

Morin (2',4',4,5,7-pentahydroxyflavone) (Scheme 1) is an important natural antioxidant and exhibits biological activity. According to recent studies,[1–4] morin plays an important role in the protection of human erythrocytes; performs antiinflammatory, antiatherosclerotic, and antistress functions; and also exhibits antiviral and anticancer activity. For the determination of morin in pharmaceutical preparations and vegetable raw materials, HPLC[5–7] and spectrophotometry[8] have been used. However, in the last decade, electrochemical analysis methods have increasingly been developed to determine flavonoids. This trend can be explained by the fact that the use of voltammetric methods enables to create selective, cheap, and miniature sensors for rapid qualitative and quantitative analysis. To determine morin, a number of voltammetric sensors were proposed. These sensors are based on a glassy carbon electrode modified with carboxylated nanotubes;[9] a composite of graphene oxide, poly-3,4-ethylenedioxythiophene, and gold nanoparticles;[10] 1-butyl-3-methylimidazoliumhexafluorophosphat and chitosan;[11] poly(tetrafluroethylene)-deoxyribonucleate acid;[12] and vanadium pentoxide.[13] Sensors developed based on a mixture of carbon nanotubes and paraffin oil,[14] renewable pencil electrodes[15], and carbon fiber paper electrode modified with poly(2,5-dimercapto-1,3,4-thiadiazole)[16] were also proposed (comparative characteristics of the proposed sensors are presented in Table 1). In the above studies it was established that, in the determination of morin, the oxidation current has a predominantly adsorptive character.[9,11,13,14] This can be explained by the presence of five hydroxyl groups in the molecule of morin, which contributes to its adsorption on the surface of the sensor due to the formation of hydrogen bonds.

*Correspondence: 270892denis@gmail.com

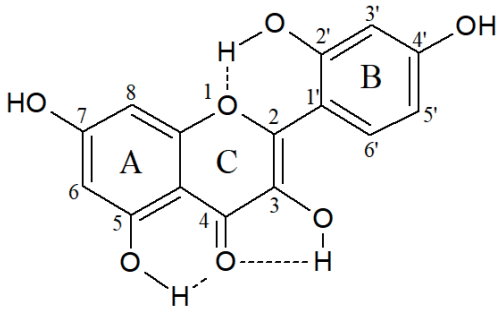

Scheme 1. Structure of morin.

Table 1. The comparative characteristics of the described voltammetric methods for the determination of morin.

Electrodes	Linear range, µM	Sensitivity, µA/µM	LOD, µM	Ref.
CPB/SWNT-COOH/GCE	0.1–100 and 100–750	0.21 and 0.10	0.029	[9]
PEDT–Au/rGO/GCE	1–20 and 20–150	0.29 and 0.062	0.0083	[10]
Ch–MWCNT/LI/GCE	3.5–40	Not given	0.054	[11]
V_2O_5 NF/GCE	0.05–11	0.080	0.0090	[13]
CNTPE	0.005–0.10	0.046	0.0010	[14]
PGE	0.095–1.3	0.17	0.025	[15]
PDMTD/CFPE	0.0028–0.00025	Not given	8.3×10^{-5}	[16]
ECA-CPE	0.16–0.80 and 0.8–6	0.56 and 0.31	0.027	This work

CFPE- Carbon fiber paper electrode; Ch- chitosan; CNTPE- multiwalled carbon nanotubes-paraffin oil paste electrode; CPB- cetylpyridium bromide; LI- ionic liquids; MWCNT- multiwalled carbon nanotube; PDMTD- poly(2,5-dimercapto-1,3,4-thiadiazole); PEDT–Au- polyethylenedioxythiophene-gold nanoparticles; PGE- renewable pencil electrode; rGO- reduced graphene oxide; SWNT-COOH- carboxylated single-walled carbon nanotubes; V_2O_5 NF- vanadium pentoxide nanoflakes.

Along with the modification of carbon-paste electrodes (CPEs), one should note their electrochemical activation.[17] It is established that during the electrochemical activation of CPEs, partial oxidation of graphite takes place with the formation of various oxygen-containing groups on the surface. This increases the hydrophilicity of the CPE surface and promotes the peeling off of the binder, increasing the effective surface of the electrode and the heterogeneous electron transfer rate constant.[17] However, the conditions for electrochemical activation strongly depend on the material and composition of the electrode. Previously, we established optimal conditions for the electrochemical activation of a CPE,[18] and a highly sensitive sensor for the determination of quercetin (a morin isomer) was developed.[19] The purpose of this paper is to investigate the electrochemical behavior of morin on an electrochemically activated CPE and to develop a voltammetric sensor for its determination.

2. Results and discussion

2.1. Electrochemical behavior of morin on ECA-CPE

To study the electrochemical behavior of morin on ECA-CPE, cyclic voltammetry was applied. Figure 1 shows the cyclic voltammograms of the morin solution recorded on the CPE and ECA-CPE. When using the ECA-

CPE, the oxidation current of morin increases by 1.85 times in comparison with untreated CPE, and the potentials of the oxidation peaks are shifted to the region of negative potentials. For ECA-CPE, three oxidation peaks at 435 mV, 590 mV, and about 1000 mV are seen on the cyclic voltammogram of morin. When the scan is repeated, the oxidation current decreases, and the potential of the first oxidation peak shifts toward more positive potentials.

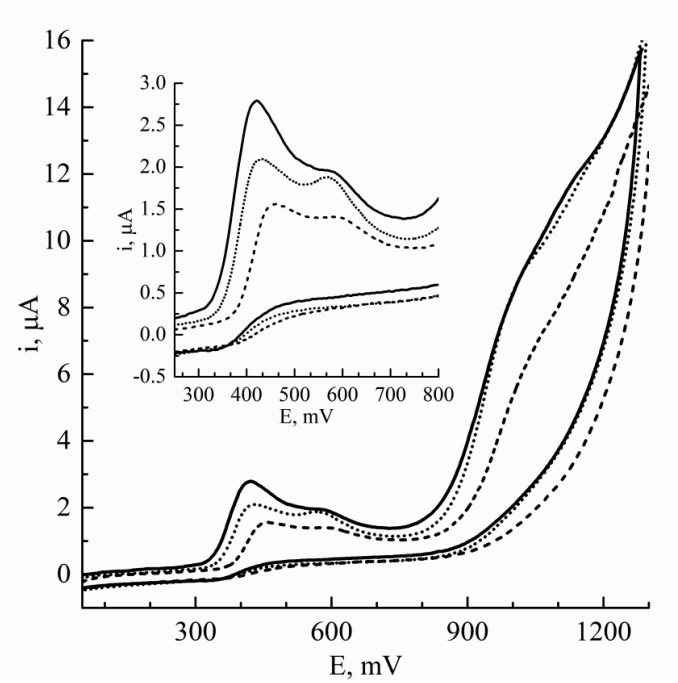

Figure 1. Cyclic voltammograms of ECA-CPE first (solid line) and second (dotted line) scan and of CPE (dashed line) in Britton-Robinson buffer solution with pH 4 containing 100 μM morin at scan rate of 50 mV s^{-1}. Inset: An enlarged fragment of the voltammograms.

This can be explained by adsorption of the products of the morin oxidation and blocking of the surface of the electrode. It should also be noted that at a low scan rate the cathodic peak corresponding to the first oxidation peak is not observed. However, at high scanning rates, the corresponding cathodic peak is observed, which may indicate a chemical interaction of one of the oxidation products resulting in the formation of a nonelectroactive compound.[20]

2.2. Effect of pH

The influence of the pH of the medium on the cathodic peak current and potential of morin on ECA-CPE has been studied. As can be seen (Figure 2), when the pH of the medium increases from 2 to 4, the oxidation current of morin increases and reaches a maximum. With a subsequent increase in pH, the oxidation current decreases and remains constant in the pH range of 5–6, and it decreases sharply in alkaline medium. At pH 4, taken as the optimum, morin in aqueous solutions is in neutral form (~71%).[21] We note that a similar dependence was obtained by studying the effect of the pH of the medium on the oxidation current of quercetin on ECA-CPE.[19]

When studying the influence of the pH of the medium on the potentials of the first and second anodic peak of morin, the following dependences ($E_{pa} = f(pH)$) were obtained: E_{pa1} = –56.42 pH + 640.2 (R^2 =

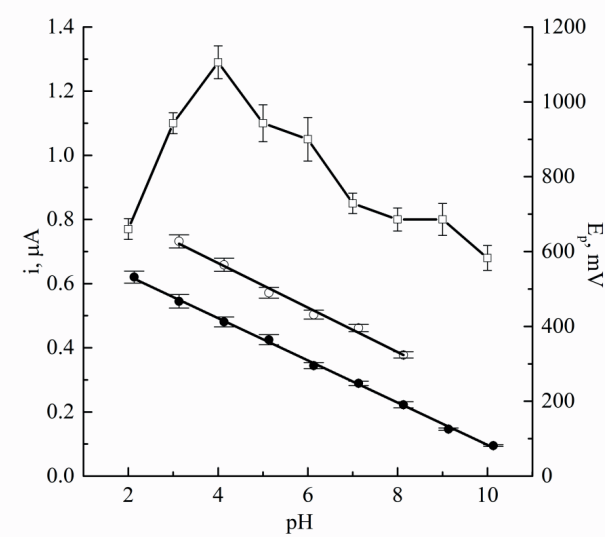

Figure 2. Plot of the oxidation peak current (left axis) and oxidation peak potential (right axis) of morin on ECA-CPE as a function of pH.

0.9990) and E_{pa2} = –59.47 pH + 799.24 (R^2 = 0.992). The number of protons (m) per electron (n) for the first oxidation peak (m/n = 0.96) and the second oxidation peak (m/n = 1.01) was calculated from the tangents of the slopes of the reduced dependences. Thus, it can be concluded that an equivalent amount of protons and electrons take part in the oxidation process.

2.3. Effect of scan rate

To determine the nature of the current and the number of electrons participating in the oxidation process, the dependence of the effect of the potential scan rate on the oxidation current of morin on ECA-CPE was studied. To determine the nature of the anodic current on ECA-CPE on the basis of cyclic voltammograms of morin at different scan rates (Figure 3a), the dependence (Figure 3b) $i = f(\upsilon)$ was constructed, which is described by the following equation: i = 0.0168 υ+ 0.353 (R^2 = 0.990). The obtained data allow us to conclude that the anodic current of morin on ECA-CPE is controlled by adsorption.

To determine the number of electrons taking part in the oxidation of morin, the dependences of $E_{pa} = f(lg\upsilon)$ were constructed for the first and second anodic peak, which are described by the following equations: E_{pa1} = 57.3 lgυ+ 315 (R^2 = 0.9901) and E_{pa2} = 123.5 lgυ+ 297 (R^2 = 0.981). Based on the slope of the dependence, $E_{pa} = f(\lg\upsilon)$ for adsorption-controlled processes ($tg\alpha = 59.05/(\alpha n)$), and considering that the charge transfer coefficient (α) for completely irreversible processes is close to 0.5,[22] the numbers of electrons for the first (n = 2.06) and the second (n = 0.97) oxidation peak were calculated. On the other hand, on the basis of the work of Laviron[23] on the adsorption-controlled current for completely irreversible systems (based on the function $G = f(\alpha n(E - E_p))$, we can conclude that the potential difference between peak and half-peak ($E_p - E_{p/2}$) for the anode current will be ($E_p - E_{p/2}$) = 37.5/(αn). In this way, the values of n are calculated for α = 0.5 for different potential scan rates. According to the obtained data, the average value of $E_p - E_{p/2}$ for the scan rate of 200 mV/s is 39.8 mV, which corresponds to n = (1.88 ±0.10) ≈ 2. With a subsequent increase in the potential scan rate, the first peak of the morin oxidation is broadened, and the average $E_p - E_{p/2}$

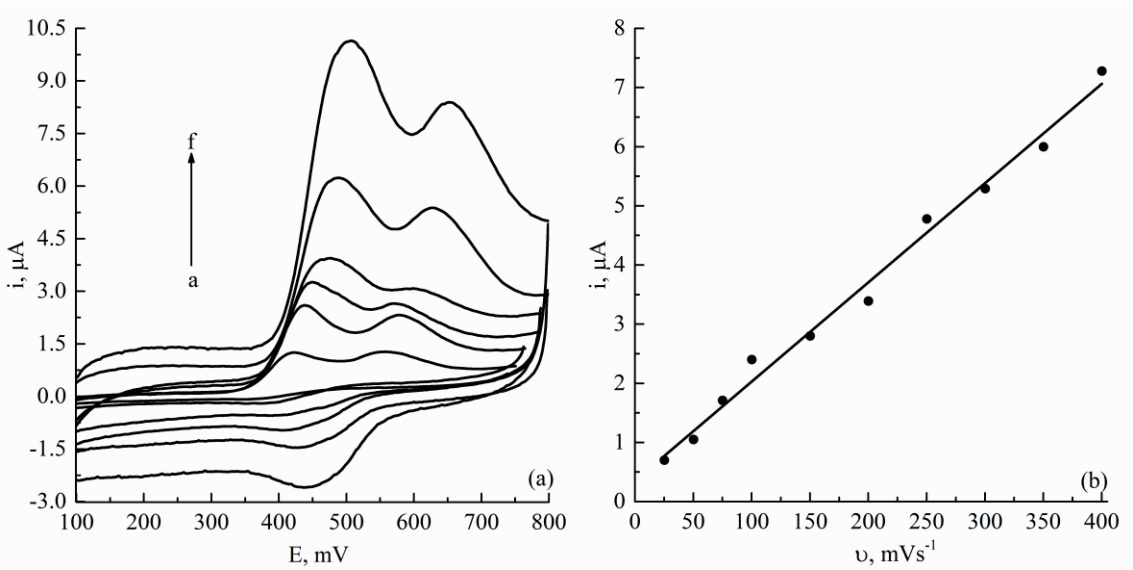

Figure 3. (a) Cyclic voltammograms of ECA-CPE in Britton-Robinson buffer solution with pH 4 containing 50 µM morin at different scan rates (from a to f): 50, 100, 150, 200, 300, 400 mV s^{-1}. (b) Plot of the oxidation peak currents of morin as a function of scan rate.

becomes 59.0 mV, which corresponds to n = (1.27 ±0.05) ≈ 1. Also, at a scan rate higher than 200 mV/s, a cathodic peak related to the first oxidation peak was observed. The calculated average difference value of the potentials of peak and a half-peak ($E_p - E_{p/2}$) for the peak that corresponds to the oxidation peak is 69.1 mV, which corresponds to n = (1.08 ±0.12) ≈ 1.

2.4. Mechanism of morin oxidation

The differences in the literature data on the mechanism of oxidation of morin and the assignment of oxidation and reduction peaks to the corresponding functional groups should be noted. Thus, in one work,[9] the authors noted two-electron consecutive oxidation of morin (pH 8) at the 4' and 3C positions, respectively. The same conclusion was reached by the authors studying the oxidation of morin on a platinum electrode.[24] Other authors observed two anodic peaks in the study of oxidation of a powder of morin mechanically fixed on the surface of a GCE.[25] One was attributed to a one-electron oxidation in ring B and the second to one-electron oxidation of hydroxyl groups in ring A.[25] On the other hand, in the oxidation of morin at a pencil graphite electrode (pH 3.25),[15] glassy carbon electrode (pH 7.28)[12], and carbon fiber paper electrode (pH 7),[16] the authors noted the presence of one two-electron oxidation peak corresponding to the oxidation of hydroxyl groups at the 4'C and 3C position of rings B and C, respectively.

Based on the data obtained, we propose the following scheme for the oxidation of morin using the ECA-CPE (Scheme 2). At low potential scan rates (up to 200 mV/s), the first anodic peak (E_{pa1} = 435 mV) can be attributed to a two-electron, two-proton reaction (ECEC mechanism). In this case, the first step is the formation of semiquinone at the 4'C position in ring B (IIa). Semiquinone (IIa) is in tautomeric equilibrium with forms IIb and IIc. However, due to the presence of a strong hydrogen bond in position $5OH \cdots O4C$ and the hydrogen bond $2'OH \cdots 1O$ symmetric to it, the formation of the tautomeric form IIb is more likely than IIc. If the potential scan rate is small in comparison with the rate of tautomeric transformation of IIa into IIb,

further oxidation is possible with the formation of intermediate IIIb, which is rearranged into IVb. The next anodic peak ($E_{p\,2}$ = 590 mV) corresponds to one electron with the transfer of one proton and refers to the oxidation of the hydroxyl group at the 2'C position to form a Vb followed by dimerization or electron transfer, etc.

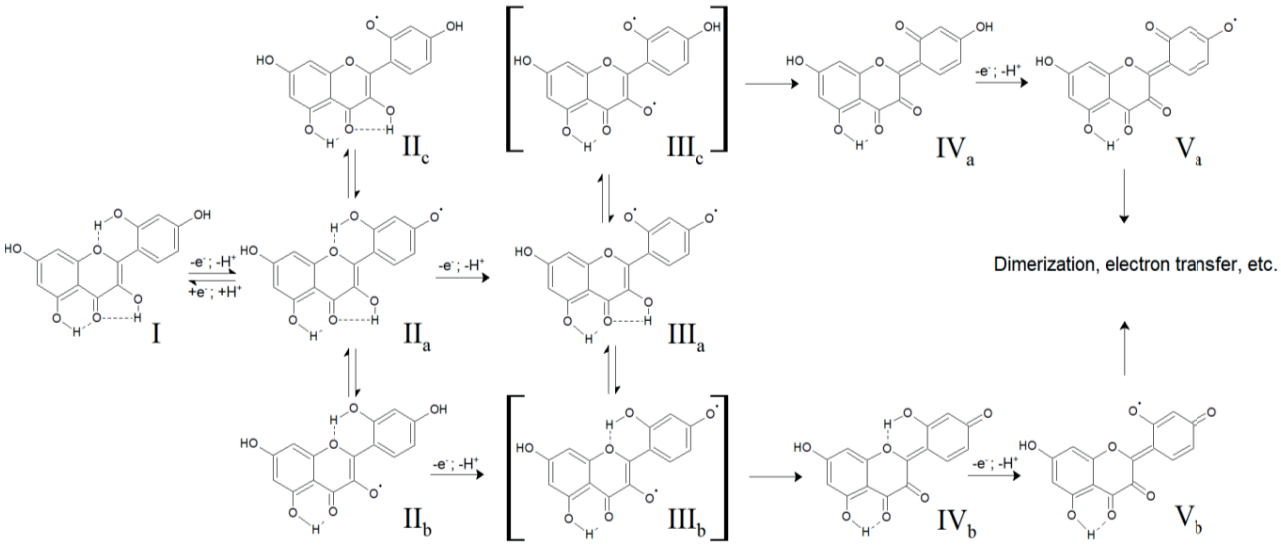

Scheme 2. Scheme of morin oxidation on ECA-CPE.

On the other hand, at a high potential scan rate, the first anodic peak (E_{pa1} = 500 mV) passes into a one-electron peak and a corresponding cathodic peak appears. It is established that this peak (E_{pa2} = 450 mV) is also one-electron and refers to the reduction of semiquinone (IIa) back into morin (I). With further oxidation, when the scan rate of the potential is greater than the rate of tautomeric conversion of form IIa to IIb, formation of intermediate form IIIa, which is also in tautomeric equilibrium with forms IIIb and IIIc, is possible. The preferential formation of form IIIb than IIIc can also be explained by the formation of a strong hydrogen bond at the $2'OH \cdots 1O$ position. Form IIIb undergoes further oxidation as described above. However, it should be noted that the formation of forms IIIc, IVa, and Va is also possible as an alternative way of oxidation.

2.5. Optimization of adsorption parameters

As the optimized adsorption parameters of morin, we have selected the adsorption potential (E_{ads}) and the adsorption time (t_{ads}). Figure 4a shows the dependence of the oxidation current of morin on the adsorption potential at adsorption time of 60 s. With an increase in the adsorption potential up to 200 mV, the oxidation current of morin increases and then sharply decreases.

The influence of the adsorption time on the current of the oxidation of morin was studied at adsorption potential of 200 mV (Figure 4b). It is established that the oxidation current of morin increases to 180 s, and after that it remains unchanged.

2.6. Optimization of determination

To determine morin, square-wave voltammetry has been chosen. As a variable parameter, at a constant value of the frequency (ν = 25 Hz), the amplitude (A) was optimized. From the dependence obtained (Figure

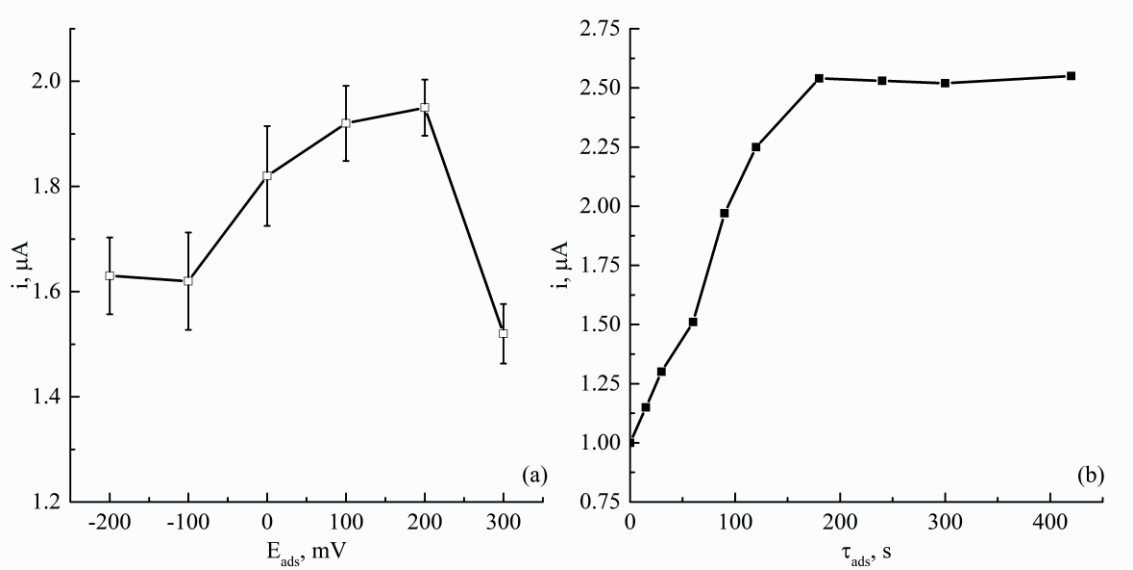

Figure 4. (a) Plot of the oxidation peak current of morin on ECA-CPE as a function of accumulation potential E_{ads} at accumulation time of 60 s. (b) Plot of the oxidation peak current of morin on ECA-CPE as a function of accumulation time τ_{ads} at accumulation potential of 200 mV.

5), it is seen that the oxidation current increases with increasing amplitude up to 35 mV and then gradually decreases. With an increase in the scan rate, the oxidation current of morin decreases, and the oxidation peak becomes wider due to the ever-increasing transition of the oxidation process to irreversible (data not shown). To determine morin, the sweep speed of 100 mV/s and amplitude of 35 mV were chosen as optimal.

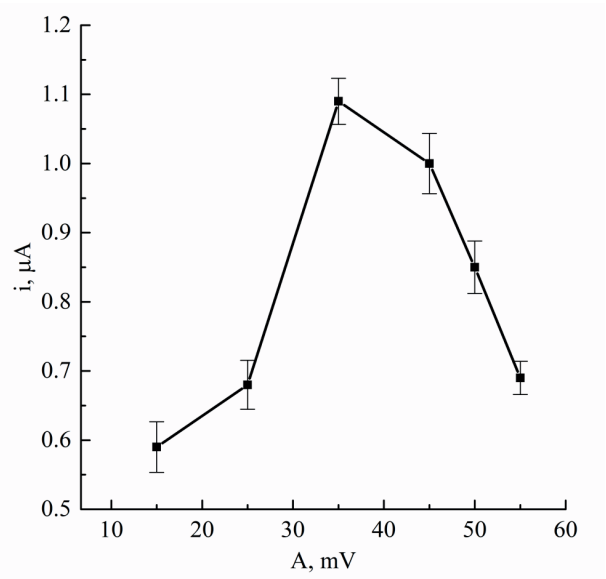

Figure 5. Plot of the oxidation peak current on ECA-CPE at 200 mV during 180 s in Britton-Robinson buffer solution with pH 4 containing 1 µM morin at different amplitudes; scan rate 100 mV s^{-1}; frequency 25 Hz.

2.7. Influence of some foreign species

The influence of foreign substances was studied in the determination of morin with a concentration of 2.5 µM in a Britton-Robinson buffer solution, pH 4. The effect of metal ions (Cu^{2+}, Pb^{2+}, Cd^{2+}, Ni^{2+}, Zn^{2+}) that can form complexes with morin was studied and they exhibited no effect on the oxidation current of morin at 100-fold excess. Rutin gives an oxidation peak on the ECA-CPE, but the oxidation potential is shifted related to the morin in the more positive potential region. Quercetin can have an effect on the oxidation current of morin, in which case sample pretreatment is necessary.

2.8. Determination of morin in model solutions and *Coffea arabica* extract

Using optimal conditions, a calibration graph was constructed for the determination of morin on ECA-CPE (Figure 6), which has two linear sections in the concentration range of morin of 6–0.8 µM and 0.8–0.16 µM, and they were described by the following equations: i[µA] = 0.314[µA/µM]·C[µM] + 0.176[µA] (R^2 = 0.993) nd i[µA] = 0.557[µA/µM]·C [µM] + 0.0221[µA] (R^2 = 0.999). The values of LOD (3σ) and LOQ (10σ) were 0.027 µM and 0.092 µM, respectively.

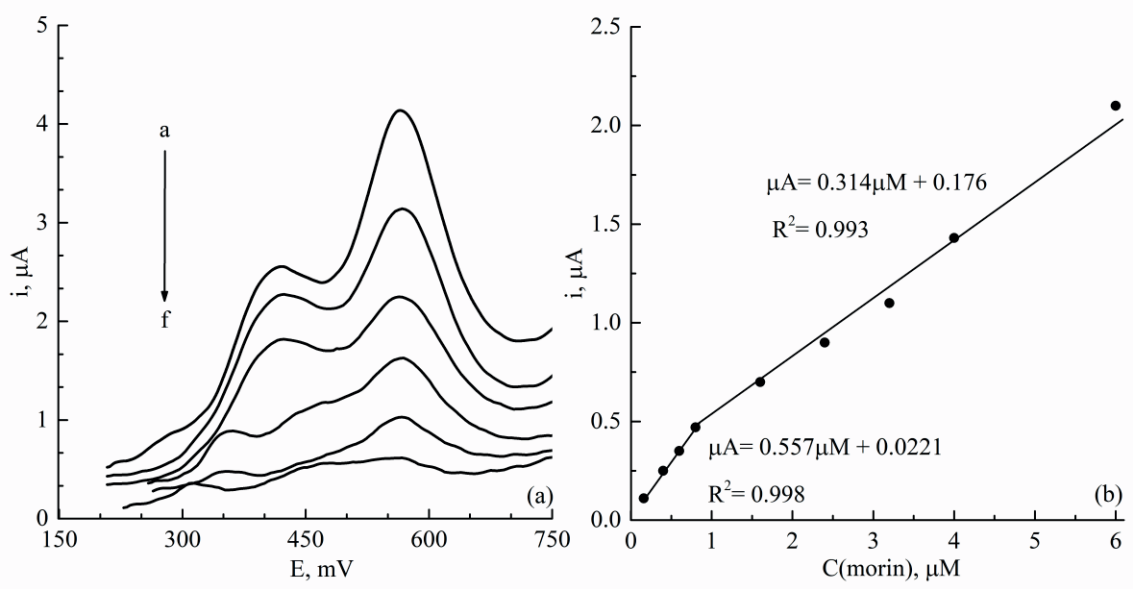

Figure 6. (a) SWVs of ECA-CPE after pretreatment at 200 mV for 180 s in Britton-Robinson buffer solution with pH 4 containing different concentrations of morin (from a to f): 6, 4, 2.4, 0.8, 0.4, 0.16 µM. (b) Plots of the peak currents as a function of morin concentration.

For validation of the proposed method, the standard additions technique was used. The reproducibility of the developed procedure was determined on the basis of 5 parallel measurements of a model solution of morin with a concentration of 1 µM, and the obtained RSD value was 4.5% (α = 0.05).

The developed technique was tested in the determination of morin in model solutions (Table 2) and . *arabica* extract (Table 3).

2.9. Conclusions

The possibility of using ECA-CPE for the determination of morin has been studied. It is established that the anodic current of morin on ECA-CPE increases by 1.85 times in comparison with unmodified CPE and has an

Table 2. Results of the determination of morin in model solution (n = 3, P = 0.95).

Added, µg	Found, µg	RSD, %
18.1	18.25 ±0.93	2.1
12.09	12.31 ±1.08	3.5
6.05	5.8 ±0.63	4.3

Table 3. Results of the determination of morin in *C. arabica* extracts.

Added, µg	Found, µg	Recovery, %
12.1	11.8	97.5
6.05	6.02	99.5
3.02	3.10	102.6

adsorption nature, and the potentials of the oxidation peaks are shifted to the region of negative potentials. When studying the oxidation of morin on ECA-CPE, it was found that at low scan rates, the oxidation of morin is irreversible followed by the transfer of two and one electrons, and at high scan rates a reversible cathodic peak corresponding to the first anodic peak appears.

Based on the data obtained, a scheme for the oxidation of morin on ECA-CPE is proposed. In optimal conditions (pH = 4, E_{ads} = 200 mV, t_{ads} = 180 s), using square-wave voltammetry (A = 35 mV, ν = 25 Hz, υ = 100 mV/s), it is possible to determine morin within 6–0.8 µM (with a sensitivity of 0.314 µA/µM) and 0.8–0.16 µM (with a sensitivity of 0.557 µA/µM). The developed sensor was tested in the determination of morin in model solutions and *C. arabica* extracts with RSD of no lower than 4.5%.

3. Experimental

3.1. Reagents and apparatus

Stock solution of morin (1×10^{-2} M) was prepared in ethanol and stored at 4 °C. Graphite powder for the preparation of the CPE was obtained from spectrally pure graphite. All other solutions were prepared using reagents of class not lower than analytical pure grade.

Electrochemical experiments were performed on voltammetric analyzer Ecotest-VA (OOO Econics Expert, Russia) with a three-electrode cell consisting of silver-chloride reference electrode EVL-1M4 (saturated KCl), an auxiliary platinum electrode EPL-02, and CPE as the work electrode.

The pH was measured by glass electrode ECL 63-07 paired with a silver-chloride reference electrode EVL-1M3 on ionomer I-160.

3.2. Preparation and electrochemical activation of CPE

The bare CPE was prepared by mixing graphite powder and silicone oil in a 4:1 ratio by weight and homogenized in a mortar. The resulting paste was placed in a polytetrafluoroethylene tube with an inner diameter of 4 mm, and a copper cylinder was used as a current collector and piston. To update the surface of electrode, a small portion of the paste was pressed through the piston, cut off, and polished with tracing paper.

The electrochemical pretreatment of the CPE was carried out in 1 M NaOH solution at 1.5 V for 120 s. The resulting ECA-CPE was thoroughly washed with distilled water.[18]

3.3. Determination of morin in *C. arabica* extract

Morin was extracted from *C. arabica* samples according to the established procedure.[26] Previously ground in a mortar, 0.2 g of the sample was transferred to a conical flask and 40 mL of hot water was added. The extraction was carried out with constant stirring for 4 min. The resulting extract was filtered into a 50-mL volumetric flask and diluted with distilled water at 25 °C.

References

1. Venu, J. G. *Pharmacogn. J.* **2013**, *5*, 123-126.
2. Zhou, Y.; Cao, Z. Q.; Wang, H. Y.; Cheng, Y. N.; Yu, L. G.; Zhang, X. K.; Sun, Y.; Guo, X. L. *Mol. Nutr. Food Res.* **2017**, *61*, 1-10.
3. Wang, J.; Zhou, X.; Liu, S.; Li, G.; Shi, L.; Dong, J.; Li, W.; Deng, X.; Niu, X. *J. Appl. Microbiol.* **2015**, *118*, 753-763.
4. Zhang, Q.; Zhang, F.; Thakur, K.; Wang, J.; Wang, H.; Hu, F.; Zhang, J. G.; Wei, Z. J. *Food Chem. Toxicol.* **2018**, *112*, 466-475.
5. Pavun, L.; Djikanovic, D.; Djurdjevic, P.; Stankov, M. J.; Malesev, D.; Ciric, A. *Acta Chim. Slov.* **2009**, *56*, 967-972.
6. Kongkiatpaiboon, S.; Tungsukruthai, P.; Sriyakool, K.; Pansuksan, K.; Tunsirikongkon, A.; Pandith, H. *J. Chromatogr. Sci.*, **2016**, *55*, 346-350.
7. Kumar, M. R.; Muralidharan, S. *J. Young Pharm.* **2015**, *7*, 194-199.
8. Bark, K.; Im, S.; Seo, J.; Park, O.; Park, C.; Park, H. *Bull. Korean Chem. Soc.* **2015**, *36*, 498-502.
9. Ziyatdinova, G.; Ziganshina, E.; Budnikov, H. *Electrochim. Acta* **2014**, *145*, 209-216.
10. Cheng, W.; Liu, P.; Zhang, M.; Huang, J.; Cheng, F.; Wang, L. *RSC Adv.* **2017**, *7*, 47781-47788.
11. Mariño, A.; Leiva, Y.; Bolaños, K.; García-Beltrán, O.; Nagles, E. *J. Electroanal. Chem.* **2015**, *759*, 153-157.
12. Wang, F.; Xu, Y.; Zhao, J.; Hu, S. *Bioelectrochemistry* **2007**, *70*, 356-362.
13. Sasikumar, R.; Govindasamy, M.; Chen, S. M.; Chieh-Liu, Y.; Ranganathan, P.; Rwei, S. P. *J. Colloid Interface Sci.* **2017**, *504*, 626-632.
14. Xiao, P.; Zhou, Q.; Xiao, F.; Zhao, F.; Zeng, B. *Int. J. Electrochem. Sci.* **2006**, *1*, 228-237.
15. Temerk, Y. M.; Ibrahim, M. S.; Kotb, M.; Schuhmann, W. *Electroanalysis* **2013**, *25*, 1381-1387.
16. Varghese, A.; Chitravathi, S.; Munichandraiah, N. *J. Electrochem. Soc.* **2016**, *163*, B471-B477.
17. Rice, M. E.; Galus, Z.; Adams, R. N. *J. Electroanal. Chem. Interfacial Electrochem.* **1983**, *143*, 89-102.
18. Chebotarev, A.; Pliuta, K.; Koicheva, A.; Bevziuk, K.; Snigur, D. *Anal. Lett.* **2018**, *51*, 1520-1528.
19. Pliuta, K.; Chebotarev, A.; Koicheva, A.; Bevziuk, K.; Snigur, D. *Anal. Methods-UK* **2018**, *10*, 1472-1479.
20. Wopschall, R. H.; Shain, I. *Anal. Chem.* **1967**, *39*, 1535-1542.
21. Chebotarev, A. N.; Snigur, D. V. *Russ. J. Gen. Chem.* **2016**, *86*, 815-820.
22. Laviron, E. *J. Electroanal. Chem.* **1979**, *101*, 19-28.
23. Laviron, E. *J. Electroanal. Chem.* **1974**, *52*, 355-393.
24. Masek, A.; Chrzescijanska, E.; Zaborski, M. *Food Chem.* **2014**, *148*, 18-23.
25. Janeiro, P.; Brett, A. M. O. *Electroanalysis* **2005**, *17*, 733-738.
26. Calderón, J. A.; Cardozo-Pérez, M.; Torres-Benítez, A.; García-Beltrán, O.; Nagles, E. *Anal. Methods-UK* **2017**, *9*, 6474-6481.